

$J = 1$ to $J = 0$ D_2 conversion in solid D-T

G. W. Collins, E. M. Fearon, E. R. Mapoles, R. T. Tsugawa, and P. C. Souers
Lawrence Livermore National Laboratory, University of California, Livermore, California 94550

P. A. Fedders

Department of Physics, Washington University, St. Louis, Missouri 63130

(Received 25 January 1991)

$J = 1$ to $J = 0$ molecular rotational time constants for $J = 1$ D_2 in solid D-T at 1.8 to 14 K have been obtained by analyzing the longitudinal relaxation times T_1 of the tritons in the same sample. The inherent time constant in the electric quadrupole theory of T_1 is a function of both the $J = 1$ T_2 and $J = 1$ D_2 concentrations. By subtracting out the $J = 1$ T_2 behavior as obtained from pure T_2 samples, the $J = 1$ to $J = 0$ D_2 time constants remain. From 10 to 14 K, the D_2 time constants are longer than those for T_2 at constant temperature by the ratio of the nuclear magnetic moments. From 1.8 to 5.3 K, the two time constants are identical at about 5 h. A time-constant minimum occurs at about 10 K for both hydrogens. A rate-equation theory of rotational catalysis by free hydrogen atoms created by the tritium radioactivity is presented.

I. INTRODUCTION

We have previously studied the triton nuclear magnetic resonance (NMR) in solid T_2 and normal D-T (actually a mixture of about 25 mol % D_2 –50 mol % DT–25 mol % T_2) at various temperatures. Of special interest were the triton rotational $J = 1$ to $J = 0$ (i.e., ortho-to-para) time constants, $\tau_J(T)$, where we were surprised to find a minimum value at about 10 K.^{1–5} This was postulated to be caused by the magnetic moments of free hydrogen atoms created by the tritium radioactivity. Such atoms have been seen in our laboratory in up to 1000 ppm concentration by electron spin resonance (ESR).⁶ As the temperature decreases, the rate of atomic recombination also decreases, but the atom concentration increases. Efficient $J = 1$ to $J = 0$ catalysis depends on both atom concentration and the atoms' speed in moving from molecule to molecule. The conditions for most efficient catalysis occur at about 10 K.

In this paper, we measure the $J = 1$ to $J = 0$ (i.e., para-to-ortho) time constants for the D_2 in D-T, as seen through the NMR of the $J = 1$ T_2 . This indirect approach is used because the zero nuclear spin of $J = 0$ T_2 allows large changes to occur in the $J = 1$ T_2 /DT-triton system. In contrast, $J = 0$ D_2 has a nuclear spin, and a direct measurement of the deuteron free-induction decay (FID) would show only a small change with the decay of $J = 1$ D_2 .

We found that the longitudinal nuclear relaxation time, T_1 , of the triton in solid D-T at 5–14 K is dominated by the electric quadrupole-quadrupole (EQQ) mechanism^{4,7} first described by Moriya and Motizuki.⁸ Their theory states that the spin-lattice relaxation time is long and that a spin-rotation mechanism actually determines the experimentally seen value. The electric quadrupole moments of neighboring $J = 1$ T_2 molecules interact and split the $J = 1$ energy level into a band. When the energy between

substates is comparable to the NMR frequency, efficient relaxation occurs. All nuclear magnetic energy, then, is funneled through the $J = 1$ T_2 . For the EQQ and NMR energies to be comparable, the $J = 1$ T_2 molecules must be several intermolecular distances of each other because the quadrupole-quadrupole interaction decreases as the inverse fifth power of the distance. Below 0.1 mol % $J = 1$ T_2 , where the $J = 1$ molecules are ten intermolecular distances apart, we may expect the EQQ mechanism to weaken and for spin-lattice relaxation to appear. We can never reach this point by waiting, as we shall see in this paper, because the tritium radioactivity constantly creates new $J = 1$ T_2 . We, therefore, expect the EQQ mechanism to be fully operational for the triton in our normal D-T samples.

We are especially interested in the relaxation time T_1 of the solid hydrogens at a temperature so low that molecular diffusion does not occur (e.g., < 10 K for H_2). We are also considering only the hexagonal-close-packed unordered state of the solid. Within this range, the EQQ theory predicts the nuclear relaxation to be temperature independent. The essence of EQQ theory is that all nuclear spins, I_j , of a given nucleus, X_j (H, D, or T), are relaxed solely by the $J = 1$ form containing that nucleus, which has a nuclear spin I_1 . The pure $J = 1$ species has an inherent spin-rotation time T_{11} , which is related to the measured relaxation time by the equation

$$T_1 = \frac{\sum [X_j] I_j (I_j + 1)}{[J = 1 X] I_1 (I_1 + 1)} T_{11}, \quad (1)$$

where $[X_j]$ is the mol % of the hydrogen and $[J = 1 X]$ is the mol % of the $J = 1$ species of that isotope. The sum of all hydrogens in the samples equals 100%. Species with zero nuclear spin are NMR transparent and do not enter into the EQQ relaxation. Equation (1) states that, for the particular sample composition, the $J = 1$ species

will lose its nuclear magnetic energy with a time constant T_{11} . However, all the nuclear magnetic energy for the same isotope is crowding out the same $J=1$ path, so that the final time constant is lengthened by the ratio of the nuclear magnetic heat capacities.

The "inherent" time constant T_{11} contains the $J=1$ dependence of T_1 and is responsible for the T_1 minimum near 1 mol % $J=1$ H_2 in solid HD.^{9,10} In the range 1 to 40 mol % $J=1$ H_2 , T_{11} shows no NMR frequency effect (for given $J=1$ H_2 values) at 9–60 MHz. Unfortunately, no data has been taken above 4.2 K. In solid H_2 , T_{11} is the same as that derived from HD. The H_2 values are the same at both 5.5 and 29 MHz and from 1.5 to 10 K.¹¹ We note that the proton and triton have the same nuclear spin and their magnetic moments are almost the same in size. Thus, we expect the triton to show virtually the same EQQ relaxation behavior as the proton.

II. PROCEDURE

To obtain the D_2 $J=1$ to $J=0$ time constant, $\tau_J(D)$, we shall turn to the triton FID in solid D-T. This FID height is the sum of those from the molecular DT and the

$J=1$ T_2 . Both relax with the same longitudinal relaxation time, T_1 . The $J=1$ T_2 converts exponentially to $J=0$ T_2 until a small residual $J=1$ T_2 signal is left, and almost all of the steady-state signal is now due to DT. The $J=1$ T_2 FID has been previously analyzed to give us the $J=1$ to $J=0$ time constant, τ_J .^{1,3} These values plus new data are listed in Table I.

Using the EQQ theory from Eq. (1), the triton's longitudinal relaxation time, T_1 , may be written

$$T_1 = \frac{3/4\{[DT] + [HT]\} + 2[J=1 T_2]}{2[J=1 T_2]} T_{11}, \quad (2)$$

where the nuclear spin of the triton in DT is $\frac{1}{2}$ and in $J=1$ T_2 is 1. The amount of HT is small—generally about 1%. The dimensionless ratio in Eq. (2) is a combination of molar concentrations with the variable quantity for any sample being the $J=1$ T_2 concentration. However, T_{11} is dependent on the sum of the $J=1$ T_2 and $J=1$ D_2 in the sample. This provides us with a means of studying the $J=1$ D_2 by way of the triton's relaxation time. To see that this is true, we consider Fig. 1, which shows the triton T_1 in D-T as a function of time

TABLE I. $J=1$ to $J=0$ time constants for tritons and deuterons in solid D-T and T_2 as measured by triton NMR. The sample numbers ending with "N" were measured at 15 MHz; all others were measured at 30 MHz.

Sample	Sample No.	Sensor temp. (K)	Correct temp. (K)	$J=1$ to $J=0$ time (h)		Deuteron time $t_J(D)$	Calc. final $[J=1 T_2]$	final $[J=1 D_2]$	thermal $[J=1 DT]$ (mol%)
				Measured triton time, $t_J(T)$	From T_1				
D-T	2N	1.5	1.8	4.8			0.5	0.3	0.0
	3N	1.5	1.8		5.0	5.1	0.5	0.3	0.0
	4N	1.5	1.8	5.6	6.0	4.6	0.5	0.3	0.0
	7N	2.5	2.6	3.3	4.8	4.0	0.5	0.3	0.0
	31	3.0	3.1		4.9	6.0	0.5	0.3	0.0
	10N	3.2	3.3	4.5	6.0	4.2	0.5	0.3	0.0
	23	3.2	3.3		4.7	7.2	0.5	0.3	0.0
	25	3.2	3.3	4.8	5.5	8.0	0.5	0.3	0.0
	7	5.2	5.2	5.6	5.2	6.0	0.5	0.3	0.0
	8	5.2	5.2		5.2	5.8	0.5	0.3	0.0
	34	8.0	8.0	2.4	2.4	2.7	0.7	0.3	0.0
	22	9.9	9.9	0.5		1.8	1.2	0.3	0.1
	33	12.0	12.0	1.2		4.5	2.2	0.3	0.4
	32	13.9	13.9	5.0		16	3.7	0.3	0.9
	T_2	6N	1.4	1.8				2.1	
5N		1.5	1.9	2.4			2.1		
8N		2.5	2.8	3.3	3.5		2.1		
9N		3.2	3.4	3.3			2.1		
9		5.3	5.4	2.2	2.5		2.1		
12		7.0	7.1	1.8		1.8	2.4		
13		8.4	8.4	1.1	1.2		3.1		
10		10.0	10.1	0.5			4.9		
14		10.0	10.1	0.5			4.9		
11		12.0	12.1	0.9			9.1		
16		13.3	13.4	2.5			12.9		
15		14.5	14.6	5.7			16.8		

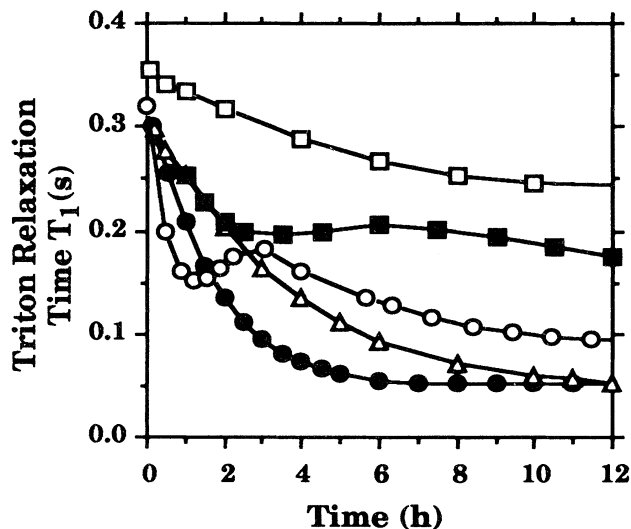


FIG. 1. The triton longitudinal relaxation time, T_1 , in solid D-T as a function of time. The presence of two different $J=1$ -to-0 times for the triton, $t_J(T)$, and for the deuteron, $t_J(D)$ is indicated by the rise in T_1 seen in the samples with corrected temperatures of 9.9 K (\circ) and 12.0 K (\blacksquare). For the colder samples at 5.2 K (\triangle) and 8.0 K (\bullet), the time constants are the same and T_1 declines uniformly. The hottest sample at 13.9 K (\square) shows only the triton time constant, whereas the deuteron time constant is too long for this plot.

(with a T_2 concentration between 24 and 31 %) at 30 MHz. Three of the samples show a smooth decline as radioactivity converts the $J=1$ T_2 to $J=0$ T_2 . The 10-K curve, however, shows a definite peak at 3 h, and the 12-K sample shows a small peak at 6 h. This shows that a second process is present. The peak means that the $J=1$ to $J=0$ D_2 conversion has an appreciably different rate than the $J=1$ to $J=0$ T_2 conversion.

We next take pure tritium T_1 data and solve for T_{11} using Eq. (2). This data is shown for the sensor temperatures 5.2, 10, and 14.5 K in Fig. 2. The lines indicate two sets of literature data by Hardy and Gaines⁹ and by Mano and Honig¹⁰ on the proton T_{11} in HD containing $J=1$ H_2 . Because of the behavior in H_2 ,¹¹ we expect no NMR frequency dependence as long as the $J=1$ concentration is greater than 1%. The triton data superimposes directly over the proton line. Because the triton and proton have nearly equal magnetic moments, we expect that the relaxation times should be almost identical unless there is an additional T_1 mechanism appropriate for the triton sample because of the radioactivity. Moving electrons, moving atoms, or complications from a badly radiation-damaged sample are all distinct possibilities. However, there is no need to appeal to any such mechanism as such a mechanism is unimportant in the present case. The pure tritium data in Fig. 2 ceases at about 2% $J=1$ T_2 because the radiation creates new $J=1$ species and a steady state occurs. In HD, one can wait for weeks

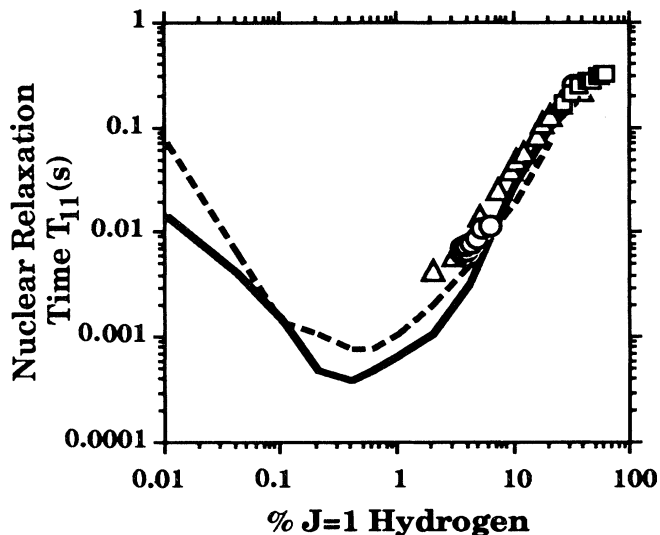


FIG. 2. Inherent longitudinal relaxation times, T_{11} , of protons in solid H_2 and tritons in T_2 as a function of the percent $J=1$ species. The lines indicate data for $J=1$ H_2 in solid H_2 : Honig at 60 MHz (—) and Hardy and Gaines at 9 MHz (---). The symbols are our $J=1$ T_2 data in solid T_2 : 5.2 K (\triangle); 10 K (\circ); and 14 K (\square). All triton data falls on the proton line. Low $J=1$ concentrations are not possible in solid T_2 because of the tritium radioactivity.

until natural catalysis causes the $J=1$ H_2 to fall to minute amounts.^{9,10} From Fig. 2, we can define the pure T_2 function

$$[J=1 T_2] = f(T_{11}), \quad (3)$$

Since our concentrations are more than a factor of 10 larger than the concentration that produces a minimum in T_{11} , we have an empirical single-valued relationship between $[J=1 T_2]$ and T_{11} . The EQQ theory predicts that, in the $J=1$ range just to the high concentration side of the minimum,

$$T_{11} \sim T_{11}(\min) + A [J=1 T_2]^{5/3}, \quad (4)$$

where $T_{11}(\min)$ is the minimum value and A is a constant.^{12,13} The 5 in the 5/3 power arises because the EQQ interaction goes as the fifth power of the distance between electric quadrupoles and the 3 because the average intermolecular spacing goes as the inverse 1/3 power of the concentration of $J=1$ molecules. At higher $J=1$ values, the power of $[J=1 T_2]$ begins to fall and finally reaches 1/2.⁹ We find that the power of 5/3 works quite well at least from 1 to 20% $J=1$ T_2 . As far as the molecular angular momentum is concerned, all species of $J=1$ molecules are very nearly identical. Thus, the relevant concentration of $J=1$ molecules for T_{11} is the total concentration of all hydrogen species. However, triton nuclei relax only via T_2 and DT molecules in their $J=1$ states. Thus, we shall next assume that the function $f(T_{11})$ holds in solid D-T. In D-T, then, we assert that

$$[J=1 T_2] + [J=1 D_2] = f(T_{11}) . \quad (5)$$

Because we already know $\tau_J(T)$ and, therefore, the $J=1$ T₂ concentration, we can subtract to get the $J=1$ D₂ concentration, $[J=1 D_2]$. By plotting this as a function of time, as shown in Fig. 3, we can derive the deuteron's $J=1$ to $J=0$ time constant. The $J=1$ D₂ conversion curves are close to being exponential, given that they are derived by subtracting two large numbers.

The pulsed NMR apparatus has been described previously. The samples comprised 0.009 mol inside a sapphire cell of 7.6-mm diameter, so that the sample is 3.8 mm thick. Using thermal conductivity data,¹⁴ we may now correct the sensor temperatures to higher values to allow for the tritium self-heating. The new average sample temperature is

$$T \approx T(\text{sensor}) + \frac{0.35 A_0 L^2}{4K} \quad (6)$$

where A_0 is the tritium self-heating of 50 000 W/m³ in solid D-T and 100 000 W/m³ in solid T₂. Also, L is the cell radius and K the thermal conductivity.¹⁵ Equation (6) assumes a one-dimensional loss of heat outward to the sapphire walls with a factor of 0.35 to account for the average.

One certainty lay in the initial percent of $J=1$ T₂ in the D-T samples at the temperature of interest. These were obtained from detailed cooling histories, and the probable $J=1$ to $J=0$ catalysis rates at each temperature. We estimate that, on the average, about one-tenth of the $J=1$ T₂ had converted to $J=0$ T₂ by the time the measurements began at the selected cryogenic tempera-

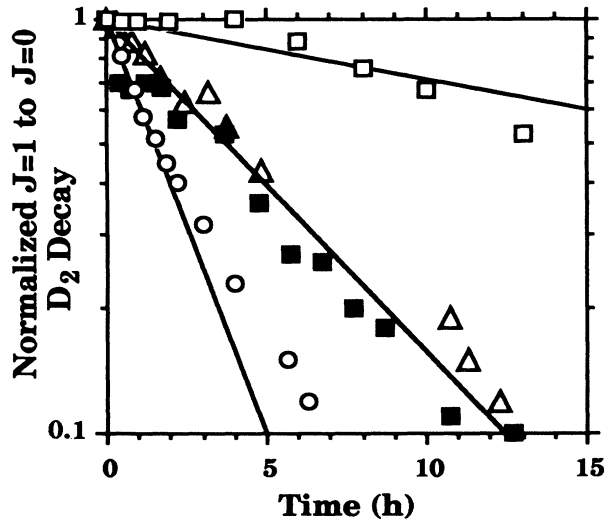


FIG. 3. Calculated decay of the $J=1$ D₂ in solid D-T as seen through the triton relaxation time, T_{11} . The corrected temperatures of these samples are 1.8 K (■); 5.2 K (△); 9.9 K (○); and 13.9 K (□). The nonexponential behavior is the result of subtracting two large numbers to obtain these results.

ture. This resulted in initial values of about 68% $J=1$ T₂ in pure tritium and 17% $J=1$ T₂ in D-T. We likewise expected about 8% $J=1$ D₂ in D-T. The old T₂ samples were 96.4% T₂ with 3% DT plus HT. The new T₂ samples (marked with an “N”) contained 98.4% T₂ with 1.3% DT plus HT. All D-T samples contained about 1% HT and 1% HD.

The endpoint $J=1$ T₂ concentrations will be further considered below because it is necessary to first obtain the $J=1$ to $J=0$ time constants. We first estimated the long-time steady-state $J=1$ compositions to be 2 mol % in pure T₂ and 0.1 mol % for both species in D-T as a result of the tritium radioactivity. This mechanism is the only dominant one at 5 K and below. As the temperature rises to 8 K and above, the measured steady-state concentration of $J=1$ T₂ in pure tritium has an increasingly large component of thermally created species. The thermally created steady-state concentration may be calculated from the partition function¹⁶

$$[J=1 T_2]_{ss,t} = \frac{9C \exp[(-57.6 \text{ K})/T]}{1 + 9 \exp[(-57.6 \text{ K})/T]} , \quad (7)$$

where 57.6 K is the energy difference between the $J=0$ and $J=1$ states of T₂. The constant C is near 100% for pure T₂ and 25% for T₂ in D-T. The actual steady-state concentration is the sum of Eq. (7) plus the amount created by radiation damage. At our higher measured temperatures, we expect the thermal mechanism to totally dominate.

Also, the thermally created amount of $J=1$ D₂ in D-T will be¹⁶

$$[J=1 D_2]_{ss,t} = \frac{75 \exp[(-86.0 \text{ K})/T]}{2 + 3 \exp[(-86.0 \text{ K})/T]} \quad (8)$$

where 25% D₂ is present in the mixture.

The creation of $J=1$ molecular DT by radiation damage may be ignored because of the instantaneous deexcitation to the $J=0$ state. However, the thermally created concentration will be¹⁶

$$[J=1 DT]_{ss,t} = \frac{150 \exp[(-71.8 \text{ K})/T]}{1 + 3 \exp[(-71.8 \text{ K})/T]} . \quad (9)$$

This amounts to 0.4% at 12 K and 0.9% at 14 K. As a result of thermal excitation, Eq. (2) becomes slightly changed to

$$T_1 = \frac{3/4\{[DT] + [HT]\} + 2[J=1 T_2]}{3/4[J=1 DT] + 2[J=1 T_2]} T_{11} , \quad (10)$$

where the $J=1$ DT now also acts as a pathway for relaxation. The small amount of $J=1$ HT may be ignored.

III. RESULTS

The results are listed in Table I. Two different $J=1$ to $J=0$ T₂ values are listed. Those “from FID” are derived by watching the decay of the time-zero FID toward a level that should represent the residual amount of DT and HT. Below 5 K, these values become doubtful because of the occurrence of “heat spikes.”¹⁷ These occur when hy-

drogen atoms suddenly recombine *en masse*, and further details will be provided in a separate paper. Their effect, however, is to lower the FID below the level expected from $J=1$ to $J=0$ conversion, so that only the part of the low-temperature data that was taken before the first sizable heat spike can be used for our present analysis.

The second conversion time listed in Table I under "from T_1 " is the $1/e$ time from a fit using Eq. (4) in the $J=1$ region just above the T_1 minimum. These time constants are not affected by the thermal spikes, but Eq. (4) does not work well at 10 K and above. This method is somewhat uncertain in pure T_2 below 5 K because the T_1 relaxation mechanism contains a separate low-temperature component, as will be described in a future paper. However, this mechanism is largest for high $J=1$ T_2 values, whereas Eq. (4) is used at low values. The low-temperature T_1 mechanism is present to a lesser extent in D-T below 5 K. We note that the agreement for $\tau_J(T)$ in Table I is good between the two derivations. The listed time constants are accurate to about $\pm 10\%$.

The derived $J=1$ to $J=0$ time constants for D_2 are also listed in Table I, with probable accuracies of about $\pm 20\%$. Both the $J=1$ T_2 and $J=1$ D_2 time constants in D-T are also displayed in Fig. 4. The results for the samples at 1.8–5.3 K are especially important, and we find these averages:

$$\tau_J(T_2 \text{ in } T_2) = 2.8 \pm 0.6 \text{ h}, \quad (11)$$

$$\tau_J(T_2 \text{ in D-T}) = 5.1 \pm 0.7 \text{ h}, \quad (12)$$

$$\tau_J(D_2 \text{ in D-T}) = 5.7 \pm 1.3 \text{ h}. \quad (13)$$

We find that the time constant for conversion of $J=1$ T_2 is twice as long in D-T as in T_2 . This seems reasonable

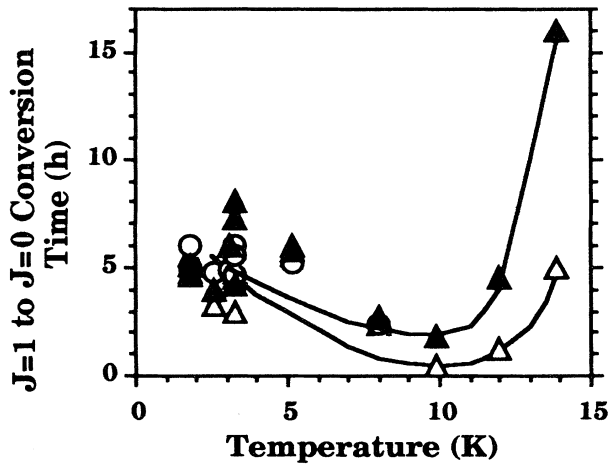


FIG. 4. Summary of $J=1$ to $J=0$ conversion times in solid D-T from 1.8 to 14 K. The triton times derived from the FID's are shown by (\triangle); those derived from T_1 analysis are given by (\circ). The deuteron times are shown by (\blacktriangle).

because of the factor of 2 in the radiation dose. We also find that the T_2 and D_2 time constants are the same. However, this seems surprising because the deuteron magnetic moment is only $\frac{1}{3}$ that of the triton, and we would expect the deuteron to be less sensitive to its environment.

For the three temperatures at 10–14 K, we find in solid D-T that

$$\tau_J(D_2 \text{ in D-T}) \simeq (3.5 \pm 0.3) \tau_J(T_2 \text{ in D-T}). \quad (14)$$

IV. CALCULATION OF THE $J=1$ ENDPOINT

Starting with the basic mechanisms of $J=1$ production and loss, we can calculate the steady state $J=1$ concentration created by the tritium radioactivity from our data. This leads us to consider the basic mechanisms of $J=1$ production and loss. Consider the basic reaction

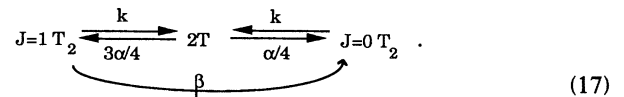


where k is the atom formation rate and α is the recombination rate. The hydrogen atom formation rate may be obtained from the rate of radioactivity decay, and for pure T_2 , it is

$$k = 2.84 \times 10^{-6} \text{ s}^{-1}. \quad (16)$$

The rate is the tritium decay fraction of 1.782×10^{-9} per second times 2 for the diatomic molecule times 156 for the average number of ion pairs created per beta particle (5685-eV beta energy and 36.6-eV per ion pair) times the 5.1 atoms created per ion pair in the gas phase.^{18–20} The rate in D-T will be $k/2$.

We are concerned with the reaction



The atom production rate is the same, but the recombination rate assumes a hot-atom equilibrium of $\frac{3}{4}$ of the recombined T_2 being $J=1$ T_2 , so that the recombination rate becomes $3\alpha/4$.²¹ The $J=1$ to $J=0$ catalysis rate, β , is just the inverse of the time constant $\tau_J(T)$. We assume that we are at 5 K and below, so that no $J=1$ T_2 is created by thermal excitation. We write the rate equations

$$d[J=1 T_2]/dt = -(k + \beta)[J=1 T_2] + (3/4)\alpha[T]^2, \quad (18)$$

$$d[T]/dt = k[T_2] - \alpha[T]^2, \quad (19)$$

where $[T]$ is the atom density. However, we shall use the brackets to mean mol % in this paper. We next assume that Eq. (19) reaches steady state quickly so that

$$\{\alpha[T]^2\}_{ss} = k[T_2] \quad (20)$$

We substitute Eq. (20) into Eq. (18) to obtain

$$d[J=1 T_2]/dt = -(k + \beta)[J=1 T_2] + (3/4)k[T_2]. \quad (21)$$

For $\beta \gg k$, the right-hand side of Eq. (21) becomes $-\beta[J=1 T_2]$, and we recognize the first-order nature of the equation. At steady state, with $\beta \gg k$ and using the time-constant format, the steady-state percent of $J=1 T_2$ is

$$[J=1 T_2]_{ss} = (3/4)k\tau_J[T_2], \quad (22)$$

where $[T_2] \approx 100$ mol %. For pure tritium, we use Eqs. (11) and (22) to obtain a calculated low-temperature steady-state concentration, $[J=1 T_2]_{ss}$, of 2.1 mol %. We have experimentally determined this concentration independently from the small long-time FID after subtraction of that part due to DT and HT. From three T_2 samples at 2.8–5.4 K, we obtain

$$[J=1 T_2]_{ss} = 2.3 \pm 0.2 \text{ mol } \%, \quad (23)$$

in excellent agreement with the calculated value. We take this as confirmation that the five atoms per molecule measured in the gas phase are likewise formed in the solid. This is critical to the ESR studies, where only a few of these atoms are seen experimentally.⁶ This result also appears to confirm the assumption of the hot atom equilibrium being created by the energy of the radioactivity decay.

We next consider D-T, where the large component of 50% DT prevents us from measuring the small long-time signal for $J=1 T_2$. We write the rate equations

$$d[J=1 T_2]/dt = -(k/2 + \beta)[J=1 T_2] + (3/4)\alpha[T]^2 \quad (24)$$

$$d[T]/dt = (k/2)\{[T_2] + [DT]/2\} - \alpha\{[T]^2 + [D][T]\}. \quad (25)$$

Only one T atom is lost in the recombination of D and T, but this reaction is twice as likely to occur as the recombination of two T atoms. We set $[D]=[T]$ and substitute Eq. (25) at steady state into Eq. (24). Equation (24) at steady state with $\beta \gg k$ and the result of Eq. (12) then becomes for D-T at 5 K and below

$$[J=1 T_2]_{ss} = (3/16)k\tau_J\{[T_2] + [DT]/2\} = 0.5 \text{ mol } \%, \quad (26)$$

where $[T_2] = 25$ mol % and $[DT] = 50$ mol %. The calculation for $J=1 D_2$ is similar except that $\frac{1}{3}$ of the D_2 is formed in the $J=1$ state. We have

$$d[J=1 D_2]/dt = -(k/2 + \beta)[J=1 D_2] + (\alpha/3)[D]^2, \quad (27)$$

$$d[D]/dt = (k/2)\{[D_2] + [DT]/2\} - \alpha\{[D]^2 + [D][T]\}. \quad (28)$$

Again, we set $[D]=[T]$ (which we have observed by ESR in D-T⁶), $\beta \gg k$ and use Eq. (13) to obtain at 5 K and below in solid D-T

$$[J=1 D_2]_{ss} = (k\tau_J/12)\{[D_2] + [DT]/2\} = 0.25\%. \quad (29)$$

These results are combined with the thermal excitation values to calculate the steady state $J=1$ values listed in Table I.

As a further test of these rate equations, we consider the formation of DT by the addition of D_2 and T_2 . We have

$$\begin{aligned} \frac{d[DT]}{dt} &= -(k/2)[DT] + 2\alpha[D][T] \\ &= \{[DT]_{ss} - [DT]\} / \tau_{ex}, \end{aligned} \quad (30)$$

where $[DT]_{ss}$ is the 50 mol % expected at steady state from the hot-atom equilibrium and τ_{ex} is the exchange time constant. We calculate that

$$\tau_{ex}(\text{expected}) = 2/k = 196 \text{ h}. \quad (31)$$

We performed this experiment by first holding a 98 mol % T_2 sample at 6 K for 20.6 h. The decrease in the triton FID showed that the $J=1 T_2$ concentration decreased from 67 mol % to 2.3 mol % over this time. Then, the sample was raised to liquefaction at 21 K, an equal amount of D_2 was added, and the sample was quenched back to the solid phase at 6 K, and the triton FID was monitored with time. By calibration with the pure T_2 , the initial D_2 - T_2 FID was calculated to be 1.4 mol % $J=1 T_2$ with no molecular DT being assumed present. This allowed the determination of the constant B relating the triton FID, $S(t)$, with the actual concentration. We then assumed that the $J=1 T_2$ decayed to 0.5 mol % with a 5.1-h time constant. We were then able to solve for the DT concentration using the equation

$$S(t) = B\{3/4[DT] + 2[J=1 T_2]\}. \quad (32)$$

The exchange reaction function for DT creation, Y , is then

$$Y = 1 - [DT]/[DT]_{ss}. \quad (33)$$

This function is plotted in Fig. 5 for various steady-state concentrations, $[DT]_{ss}$. The expected hot-atom (infinite temperature) equilibrium with 49 mol % DT produces a $1/e$ time constant of

$$\tau_{ex} = 280 + 50, \quad -30 \text{ h}, \quad (34)$$

slightly longer than the value predicted by Eq. (31). The thermal equilibrium at 6 K of 18 mol % DT (Ref. 22) is also shown in Fig. 5. It is clearly nonexponential and the values of Y go negative at long times, so that a thermal equilibrium does not appear possible. A 200-h time constant in agreement with Eq. (31) would occur for a 35 mol % steady-state DT concentration, which would occur at a temperature of 12 K. At this time, however, we lean toward a probable hot-atom equilibrium with the thermal endpoint being definitely unlikely.

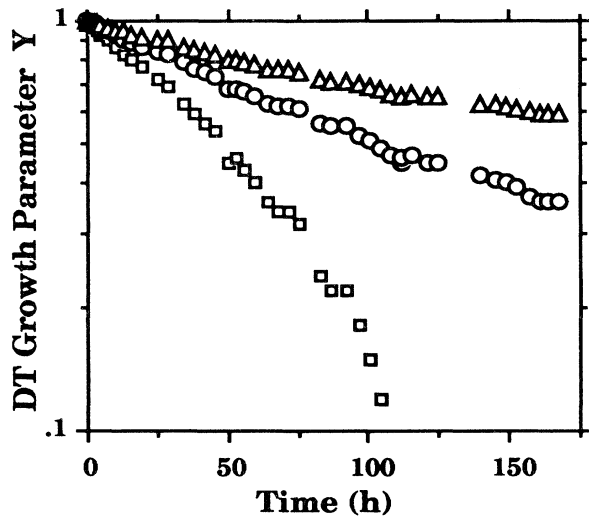


FIG. 5. Exchange reaction function, Y , which describes the formation of DT from D_2 and T_2 as a function of time at 6 K. Several postulated equilibria are shown. These are hot-atom (infinite temperature) (Δ); 20 K (\circ); and thermal at 6 K (\square).

V. DISCUSSION

We may now turn to the cause of the temperature behavior seen in Fig. 4. We first note that the mechanism for $J=1$ to $J=0$ conversion in H_2 and D_2 is the bimolecular process whereby the magnetic moment of one nucleus creates a magnetic field gradient at another nucleus.²³ The process is much faster in tritiated solid hydrogen and the reason is almost certainly because of the large magnetic field gradients generated by the free hydrogen atoms.¹ The conversion time is qualitatively thought to be dependent on two times. One is the time for the atom to hop to a new site in the crystal, and the other is the time for the atom to convert the $J=1$ molecule that it finds at its new site. At low temperatures, there are many atoms because their diffusion and recombinations are slow. At high temperatures, the atom density is low but the diffusion rate is high. The atom density and the diffusion rate are maximized at about 10 K, where the minimum T_1 values are found.

We rewrite Eq. (21) in the simplified form, useful for the first decade of $J=1$ decay:

$$d[J=1]/dt = -[J=1]/\tau_J, \quad (35)$$

where $[J=1]$ is the concentration of either $J=1$ T_2 or $J=1$ D_2 . The time constant may be written as

$$\tau_J = R_0 / (3\pi d^2 q D n), \quad (36)$$

where R_0 is the intermolecular distance of 3.6×10^{-10} m, πd^2 the cross section, q the conversion probability at a single site, D the diffusion coefficient,²⁴ probably of the hydrogen atoms, which should be more mobile than the

molecules, and n is the total D plus T atom concentration per unit volume. Equation (36) is obtained from the basic relation that the time constant is inversely proportional to the conversion cross section times the mean particle velocity. We then substitute the gas-phase relation that relates mean velocity with the diffusion coefficient and the mean free path. In solid-state reactions, the mean free path is often taken to be a constant of order R_0 . This preserves the exponential nature of the rate equation, which is found by experiment. We shall set d equal to R_0 for further simplification.²⁵

Now, in order for Eq. (36) to be first order, n must be constant. The D plus T atom densities have been measured in solid D-T and T_2 by electron spin resonance at 9.4 GHz.⁶ The atom density increases with the function

$$n = (k/\alpha)^{1/2} \tanh[(k\alpha)^{1/2}t] + ct, \quad (37)$$

where t is time, k is the radiation-driven rate of hydrogen atom formation, α is the recombination rate (per unit volume) and ct produces a linear increase seen at longer times. The atom formation curve is shown in Fig. 6 for D-T samples studied at 3–5 K. The formation rate of atoms is so fast that half of them are present by the time the sample has stabilized at the desired temperatures, so that the time t is not easy to define. Figure 6 also shows the $J=1$ to $J=0$ conversion, as determined from the FID's, for $J=1$ T_2 in D-T at 3–5 K. We see that the time for the saturation of the tanh function in Eq. (37), i.e., where the rapid increase turns into the slow linear region, is approximately equal to τ_J . We see that n is nearly but not exactly constant, but it is certainly not exactly so. This introduces a definite uncertainty into our model,

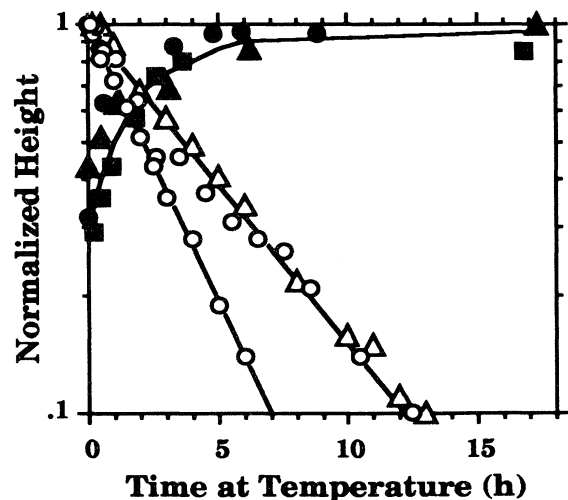


FIG. 6. Comparison of $J=1$ to $J=0$ conversion curves for $J=1$ T_2 (open symbols) and growth of all hydrogen atoms (closed symbols) in solid D-T at 3 to 5 K. The conversion curves are derived from the FID's, and the atom data is obtained from electron spin resonance. The nominal temperatures are 3 K (\circ); 4 K (\square); and 5 K (Δ).

because the actual conversion $J=1$ T_2 curves appear exponential.

Table II lists smoothed and interpolated hydrogen atom data as derived from ESR at 9.4 GHz. The atom densities are listed in parts per million at all the temperatures where $J=1$ to $J=0$ data has been taken.^{5,26} The densities in ppm may be converted to atoms/m³ using solid densities of 53 000 and 51 500 mol/m³ for solid D-T and T_2 , respectively.²⁷ The quantity n_{sat} is the total atom density at the point at which the tanh function behavior in Eq. (37) converts into the linear behavior. For both solid D-T and T_2 from 1.8–5 K, the data may be approximated by

$$n_{\text{sat}} \sim 56 \exp[(6.4 \text{ K})/T] \text{ ppm} . \quad (38)$$

The measured time at n_{sat} is τ_{sat} . We assume that the time constant for the tanh function, τ_a , occurs at $0.76n_{\text{sat}}$ and we list this time as well. The intent of listing these times is to allow comparison with the conversion times, τ_J . We see that $\tau_a < \tau_J(T)$ in most cases.

We first note that the $J=1$ to $J=0$ energies of 57.6 K for T_2 and 86.0 K for D_2 are less than the 100 K Debye temperature of solid hydrogen.²⁸ The conversion can, therefore, take place in either hydrogen with a single phonon process, and we expect no isotopic effect because of the phonon spectrum.

Next, we shall try to explain why we obtain different temperature behavior for the conversion time constants as shown in Fig. 4. We shall consider the assumption that the conversion probability q is a function of the length of time that a hydrogen atom spends at a particular site. We postulate the simple function

$$q = 1 - \exp(-t_d/t_0) , \quad (39)$$

where t_d is the average time that an atom spends at one site. It is related to the diffusion coefficient by the relation

$$t_d \approx R_0^2/4D . \quad (40)$$

The other constant t_0 is the shortest site time for which q is just one. It is obtained from the diffusion coefficient at about 8 K, where $\tau_J(T) \sim \tau_J(D)$. At 8 K and below, we can calculate

$$D = 1/\{3\pi R_0 \tau_J n\} . \quad (41)$$

We return to consider Eq. (39). At temperatures below 8 K, $t_d \gg t_0$, so that $q \approx 1$. Then, an atom converts all the $J=1$ molecules around it on each hop whether they are T_2 or D_2 so that the conversion time constants are the same. The diffusion coefficient decreases with temperature, while the atom density increases so that the temperature dependence of τ_J is slight. Above 8 K, $t_d \ll t_0$, and we use the expansion $\exp(-x) \sim 1-x$ in Eq. (39) to obtain $q \sim t_d/t_0$, so that

$$qD = R_0^2/4t_0 . \quad (42)$$

The product of qD is a constant and the diffusion coefficient does not enter into the description. Using Eq. (36) at the higher temperatures, τ_J is a function only of the atom concentration and the diffusion coefficient cannot be obtained from the data. The rapid increase of τ_J with increasing temperature must be caused by the decrease in atoms available for catalysis. This concentration decrease is caused by the increased diffusion coefficient and the increased recombination of the atoms. We must note, however, that the function in Eq. (39) is the simplest model and may not be completely correct.

At about 8 K, we postulate that q is just equal to one. The hopping time is calculated to be

$$t_0 \approx 0.6-3 \text{ s} . \quad (43)$$

It is important to note that the hopping frequency at our temperatures is on the order of 1 Hz, far below the NMR

TABLE II. Calculation of hydrogen atom diffusion coefficients using the assumption that the conversion probability is a constant equal to one. Smoothed and interpolated hydrogen atom ESR data is included. The numbers in parentheses are powers of ten.

Hydrogen	Temperature (K)	$J=1$ T_2	Time	Time	Atom	Calculated diffusion coefficient D (m ² /s)
		Time, $\tau(T)$ (h)	constant τ_a (h)	constant τ_{sat} (h)	density n_{sat} (ppm)	
D-T	1.8	5.2	1	2	2000	7(-22)
	2.6	4.0	2	4	660	3(-21)
	3.2	5.6	2	5	410	3(-21)
	5.2	5.6	1	2.5	190	7(-21)
	8.0	2.5	1.5	3	150	2(-20)
T_2	1.8	2.3	1	2	2000	2(-21)
	2.8	3.3	2	4	550	4(-21)
	3.4	3.3	2	5	370	6(-21)
	5.4	2.2	1	2.5	190	2(-20)
	7.1	1.8	1	3	80	5(-20)
	8.4	1.1	1.5	3	50	1(-19)
	10.0	0.5	2	3.5	30	

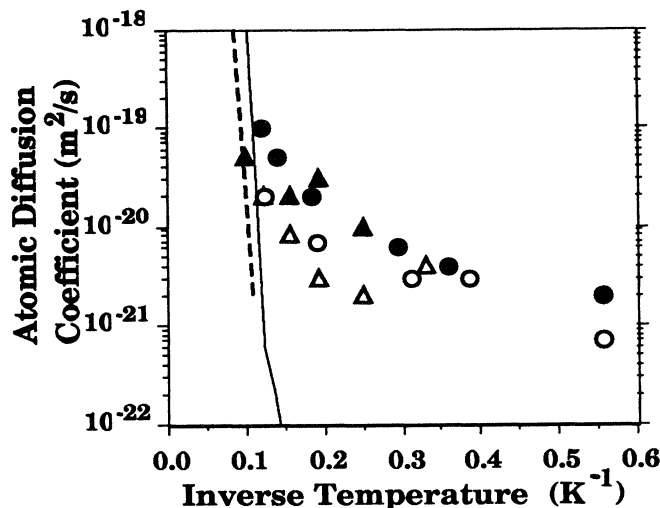


FIG. 7. Calculated diffusion coefficients from the $J=1$ to $J=0$ conversion data in this paper for hydrogen atoms in solid D-T (\circ) and T_2 (\bullet) at 1.5 to 8.4 K. Similar data from atom recombination ESR studies is indicated for solid D-T (\triangle) and T_2 (\blacktriangle). The solid line is the Soviet data for D atoms in undamaged D_2 crystal (Ref. 29). The dashed line is molecular diffusion coefficient data in solid D_2 (Refs. 30 and 31).

frequency. It does not appear, therefore, that atomic hopping can be a direct mechanism for nuclear relaxation.

We return to Table II, where we list the diffusion coefficients calculated using Eq. (41). We plot the results in Fig. 7. Also plotted are diffusion coefficients from ESR using measured atom recombination rate constants in $m^3/\text{atom s}$.⁶ We see that the two sets of data are in good agreement. For comparison in Fig. 7, we show two other curves. The solid line is measured data for D atoms in undamaged solid D_2 , where the atoms were created by gas phase discharge.²⁹ The dashed line is molecular diffusion data taken by NMR for undamaged D_2 crystals.^{30,31}

We may note two important observations from Fig. 7. First, the molecular and atomic diffusion coefficients are the same in an undamaged crystal above about 8 K, as first noticed by Ishovskikh *et al.*²⁹ This is because both atoms and molecules have to cross the 280-K energy bar-

rier to move between molecules packed at theoretical density. At low temperatures, however, the thermal energy for activation of atomic diffusion is not available. From 1.8–4 K, we find that our data fits the equation:

$$D \approx 2 \times 10^{-20} \exp[(-5 \text{ K})/T] \text{ m}^2/\text{s} . \quad (44)$$

We believe that the small 5-K activation energy probably represents quantum tunneling of the atom from site to site in the crystal. Ishovskikh *et al.* determined diffusion coefficients for D atoms in solid D_2 by ESR.²⁹ They observed the same rapid decrease of the diffusion coefficient shown in Fig. 7 at the higher temperatures followed by a leveling off at $10^{-23} \text{ m}^2/\text{s}$ below about 5 K. This behavior was attributed to quantum diffusion. It occurs two to three orders of magnitude below the tritiated results of Fig. 7, so that the radiation damage quite possibly is making atomic diffusion easier.

We return to consider Eq. (14), which compares the deuteron and tritium $J=1$ to $J=0$ time constants at the higher temperatures of 10–14 K. In this temperature regime, the atom does not reside long enough beside a $J=1$ molecule to ensure conversion, so that the $J=1$ to $J=0$ time constants should be inversely proportional to the square of the electron magnetic moment times the nuclear magnetic moment.³² We would expect the coefficient in Eq. (14) to be about 10, representing the square of the nuclear magnetic moments. We are not able to explain why the observed values are smaller.

Finally, we note from Eqs. (11) and (12) that, at 5 K and below, the $J=1$ T_2 conversion time is half as long in T_2 as in D-T. However, ESR measurements show that the atom densities are comparable at the same temperatures in the two hydrogens, and one suspects that the diffusion coefficients are also comparable. The answer is unknown, but we may postulate that twice as many ESR-invisible atoms exist in T_2 as in D-T.

ACKNOWLEDGMENTS

We would like to thank Chris Gatrousis and Tom Sugihara of the Chemistry & Materials Science Department and John Nuckolls and John Holzrichter of the Institutional Research & Development Fund for their support of this work. Work was supported by the U.S. Department of Energy by the Lawrence Livermore National Laboratory under Contract No. W-7405-ENG-48.

¹J. R. Gaines, J. D. Sater, E. M. Fearon, P. C. Souers, F. E. McMurphy, and E. R. Mapoles, Phys. Rev. Lett. **59**, 563 (1987).

²Y. Cao, J. R. Gaines, P. A. Fedders, and P. C. Souers, Phys. Rev. B **37**, 1474 (1988).

³J. R. Gaines, J. D. Sater, E. M. Fearon, P. C. Souers, F. E. McMurphy, and E. R. Mapoles, Phys. Rev. B **37**, 1482 (1988).

⁴P. C. Souers, E. M. Fearon, E. R. Mapoles, J. D. Sater, G. W.

Collins, J. R. Gaines, R. H. Sherman, and J. R. Bartlit, Fusion Technol. **14**, 855 (1988).

⁵J. R. Gaines, P. C. Souers, E. M. Fearon, J. D. Sater, and E. R. Mapoles, Phys. Rev. B **39**, 3943 (1989).

⁶G. W. Collins, P. C. Souers, J. L. Maienschein, E. R. Mapoles, and J. R. Gaines (unpublished).

⁷J. R. Gaines and P. C. Souers, in *Advances in Magnetic Resonance*, edited by J. S. Waugh (Academic, Orlando, FL, 1988),

- Vol. 12, pp. 91–112.
- ⁸T. Moriya and K. Motizuki, *Prog. Theor. Phys.* **18**, 183 (1957).
- ⁹W. N. Hardy and J. R. Gaines, *Phys. Rev. Lett.* **17**, 1278 (1966).
- ¹⁰H. Mano, Ph.D. thesis, Syracuse University (University Microfilms, Ann Arbor, MI 48106, 1978).
- ¹¹F. Weinhaus and H. Meyer, *Phys. Rev. B* **7**, 2974 (1973).
- ¹²C. C. Sung, *Phys. Rev.* **167**, 271 (1968).
- ¹³A. B. Harris, *Phys. Rev. B* **2**, 3495 (1970).
- ¹⁴G. W. Collins, P. C. Souers, E. M. Fearon, E. R. Mapoles, R. T. Tsugawa, and J. R. Gaines, *Phys. Rev. B* **41**, 1816 (1990).
- ¹⁵P. C. Souers, *Hydrogen Properties for Fusion Energy* (University of California, Berkeley, 1986), pp. 105–107.
- ¹⁶Reference 15, p. 24.
- ¹⁷G. W. Collins, E. M. Fearon, J. L. Maienschein, E. R. Maples, R. T. Tsugawa, P. C. Souers, and J. R. Gaines, *Phys. Rev. Lett.* **65**, 444 (1990).
- ¹⁸Reference 15, pp. 206, 208, 232–235, 245.
- ¹⁹D. Combecher, *Radiat. Res.* **84**, 189 (1980).
- ²⁰W. M. Jones and D. F. Dever, *J. Chem. Phys.* **60**, 2900 (1974).
- ²¹The hot atom equilibrium actually consists of 3/4 odd- J T_2 , but we assume that the excited rotational states instantly de-excite to the ground $J = 1$ level.
- ²²Reference 15, p. 296.
- ²³Reference 15, pp. 311–315.
- ²⁴Reference 15, pp. 241 and 242.
- ²⁵In Ref. 2 this theory was presented with the equation $R = cz\Omega_0\Gamma/(z\Omega_0 + \Gamma)$, where R was the $J = 1$ to $J = 0$ conversion rate, c the concentration of unpaired electron spins, Γ the rate for an electron spin to hop to a single neighboring site, z the number of neighboring sites, and Ω_0 the conversion rate for a single molecule next to an electron spin. This equation is equivalent to saying that the time to convert a $J = 1$ molecule is the sum of an atom hopping time (to come close enough) plus an interaction time (while the atom is there). Equations (35) and (36) in this text are slightly different. Besides being in the framework of reaction kinetic theory, only the hopping time of the atom (as derived through the diffusion coefficient) is important. While the atom is at rest next to a $J = 1$ molecule, there is a probability, q , that the conversion will take place. Thus, the conversion time itself is incorporated into the hopping time in this approach. With this theory we may directly move to the calculation of the diffusion coefficient.
- ²⁶The atom density, n , as measured by 9.4 GHz ESR includes atoms four or more intermolecular distances apart. If closer, their ESR linewidth would have been too broad to have been measured. We must assume the presence of “ESR-invisible” atoms at some level, but no information is available at this time. The presence of additional atoms would affect the calculated value of the diffusion coefficient.
- ²⁷Reference 15, p. 80.
- ²⁸Reference 15, pp. 99–101.
- ²⁹A. S. Ishovskikh, A. Ya. Katunin, I. I. Lukashevich, V. V. Sklyarevskii, V. V. Suraev, V. V. Filippov, N. I. Filippov, and V. A. Shevtsov, *Zh. Eksp. Teor. Fiz.* **91**, 1832 (1986) [*Sov. Phys. JETP* **64**, 1085 (1986)].
- ³⁰Reference 15, p. 88.
- ³¹F. Weinhaus, H. Meyer, S. M. Myers, and A. B. Harris, *Phys. Rev. B* **7**, 2960 (1973).
- ³²A. J. Berlinsky and W. N. Hardy, *Phys. Rev. B* **8**, 5013 (1973).